Journal of Applied Polymer Science

The Influence of Consolidation and Artificial Weathering on All-PP Composite Behavior

Alessio Ferluga, Marco Caniato, Orfeo Sbaizero
Department of Engineering and Architecture, University of Trieste, Via A. Valerio 6/A, 34127 Trieste, Italy
Correspondence to: A. Ferluga (E-mail: aferluga@units.it)

ABSTRACT: The purpose of this work was to evaluate the effect of consolidation parameters on the mechanical properties of all-polypropylene composites. Consolidation time does not induce any significant influence, whereas processing temperature and in particular coextruded tape characteristics deeply affect laminate performance. The DSC analysis demonstrated that the proximity of copolymer and homopolymer melting points results in a reduction in the operating window. This suggests the implementation of a more effective temperature control during thermoforming to avoid reinforcement relaxation and localized melting. Artificial weathering was conducted under noon summer light condition to assess the effect of ultraviolet exposure on laminates. After 100 and 250 h, sample performance drops significantly, with overall strength and elongation reduction up to 70 and 88%, respectively. Low molecular weight by-products were identified using Raman spectroscopy on specimens surface, confirming the mechanical property decrement due to photo-oxidation process. © 2014 Wiley Periodicals, Inc. J. Appl. Polym. Sci. **2015**, *132*, 41283.

KEYWORDS: degradation; mechanical properties; spectroscopy; textiles; thermoplastics

Received 7 March 2014; accepted 11 July 2014
DOI: 10.1002/app.41283

INTRODUCTION

Self-reinforced polymeric materials (SRPMs) have been widely studied over the last two decades due to their excellent mechanical properties and low density. For applications where weight is a matter of concern, SRPMs compete with traditional glass fibre composites in terms of specific strength and Young's modulus.[1] Furthermore, they can be entirely melted down allowing a complete recyclability since both matrix and reinforcements are composed of the same base material.[2] Among this material family, all polypropylene (all-PP) composites have gained attractiveness for automotive industry and road safety manufacturers since the compliance with European Directive concerning product sustainability and waste disposal costs has become more and more compelling.[3]

Self-reinforced polypropylene (SRPP) can be classified as single or multicomponent, considering the type of reinforcement and fabric weave style.[1,4,5] Single-component SRPP is completely composed of oriented PP molecules, which are partially melted and recrystallized to create the matrix.[6] During hot compaction, several layers of single component SRPP fabric are subjected to pressure and then heated up until the external skin of the material melts.[7,8] Despite narrow processing window, compacted sheets reveal excellent tensile properties. Multicomponent materials are composed of oriented polypropylene core with a lower melting point copolymer cap, resulting in a wider temperature-processing window. After consolidation, copolymer forms the matrix while the oriented phase constitutes the reinforcement of multicomponent all-PP composites.

Ward et al. have investigated the reinforcement type influence on the final properties of consolidated sheets.[9] When compared with flat coextruded tapes, multifilament bundles reveal a lower adhesion between fabric layers while fibrillated tapes exhibit a higher degree of crimp, which is detrimental for the mechanical properties of laminates.

Coextruded tape properties are affected also by drawing process, in particular by draw ratio (λ) and temperature.[10] For $\lambda \leq 9$, the orientation of both amorphous and crystalline regions causes an increase in tensile modulus, strength and shrinkage, but the fracture deformation decreases and the material density remains constant. For higher draw ratio ($\lambda > 9$), tensile modulus further increases, while both density and shrinkage decrease. This behavior is due to the orientation of the amorphous phase, which generates microvoids within the tape, but at the same time a well-packed configuration, more stable from a thermal point of view. Strength and elongation are not influenced by this mechanism. The draw temperature influences the relaxation of the oriented amorphous areas. An increment of this temperature results in higher density, lower tensile modulus, and shrinkage, while the effect on strength and elongation is not relevant. Laminates composed of coextruded tape fabric have

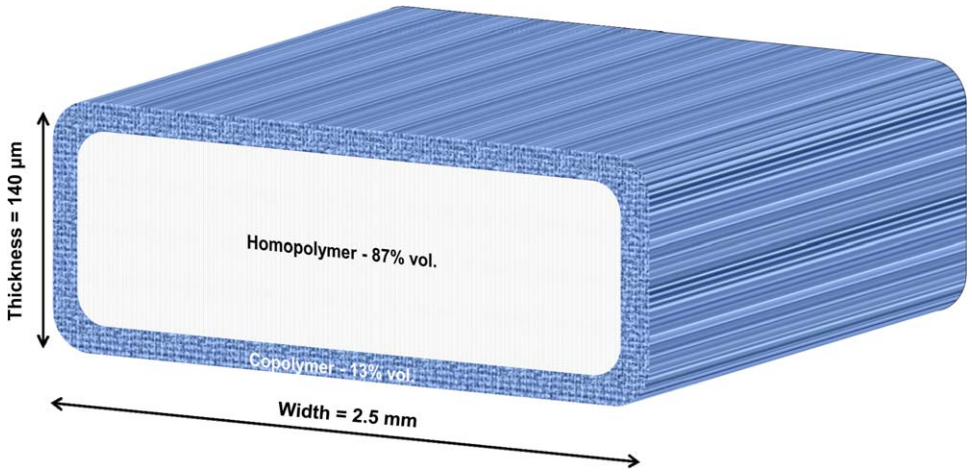

Figure 1. Schematic of coextruded PP tape cross section: homopolymer volume fraction (lighter area) is approximately 87% while copolymer (darker area) is homogeneously distributed around the oriented core. [Color figure can be viewed in the online issue, which is available at wileyonlinelibrary.com.]

shown the minimum content of intertape voids and at the same time the lowest degree of crimp, which is directly responsible for the loss of properties caused by off-axis load component.

It is important to note that weaving geometry has a significant role on the structural properties of polypropylene composites, too.[5] The void content within the fabric changes as a function of weaving parameters, such as float length, fiber density, and interlace points. Satin pattern shows the best properties followed by twill and basket; instead, plain weave style exhibits poor mechanical characteristics.

One of the most important concerns for outdoor applications (e.g., road barriers) is the mechanical property degradation caused by atmospheric agents such as water absorption and UV radiation. Even if water absorption seems to not alter the consolidated material performance, UV light affects considerably the polypropylene final properties.[11] Light absorption, through photo-oxidation reactions, induces the formation of free radicals within the polymer promoting the creation of low molecular weight by-products.[12] It has been shown that cracks observed on melted spun PP fiber surface after weathering can be directly related to the formation of carboxylic acids, esters and ketones, as discovered by FTIR spectroscopy respectively in the range 1713–1709 and 1736–1726 cm^{-1}. The resulting embrittlement and surface cracking are the major causes for the reduced mechanical strength.

Ding et al. have evaluated how irradiance intensity induces different degradation mechanisms in PP filament yarns exposed to the same cumulative energy.[13] For intensity of 81.58 and 162.58 W m^{-2}, FTIR analysis has demonstrated maximum adsorption peak around 1712 cm^{-1} typical for carbonyl group of carboxylic acids, whereas at 325.24 W m^{-2} a frequency of 1733 cm^{-1} corresponds to carbonyl group of esters. Only artificial weathering with lower irradiance levels exhibits the same kinetic of outdoor conditioned material.

Raman spectroscopy has also been performed in order to assess photo-oxidation by-products because it is sensitive for the identification of species characterized by vinyl groups.[14–18]

The aim of the present work is to evaluate the mechanical properties of coextruded tapes as well as hot consolidated all-PP composites as a function of process parameters. Consolidated sheets that have been exposed to controlled UV irradiation were assessed using Raman spectroscopy to identify the nature of weathering by-products and their influence on tensile properties.

EXPERIMENTAL

Materials Consolidation

A commercial plain weave fabric was used as base material. The same volume fraction of reinforcement was arranged in warp and weft direction for an overall fabric weight of 107 g m^{-2}. Coextruded tapes (width 2.5 mm, thickness 140 μm) had $A : B : A$ configuration (where A is PP–PE copolymer and B is oriented PP).[10] Coextruded tape cross section is outlined in Figure 1. Thermal consolidation was carried out arranging nine layers of fabric in a mold at constant pressure of 0.4 MPa.

The chosen assembly was heated at different temperatures (140, 145, and 150°C), lengths of time (300, 600, and 900 s) and then cooled at room temperature in calm air while maintaining constant pressure. Samples for artificial weathering conditioning were manufactured following the same procedure using 13 material layers. All-PP laminates have dimensions of 130 × 270 mm and thickness of 1.37 ± 0.11 mm, respectively. In Figure 2, qualitative temperature and pressure curves as a function of time are illustrated.

Sample Nomenclature

Laminates were identified (Table I) by number of layers, consolidation temperature and time. Consolidation time was kept constant for samples subjected to artificial weathering.

Tensile Test

All tensile tests were performed in compliance with ISO 527 at room temperature using Shimadzu AG-10TA universal test machine with a crosshead speed of 2 mm min^{-1}. The system was controlled by customized software, which recorded the applied load and elongation at the frequency of 3 Hz.

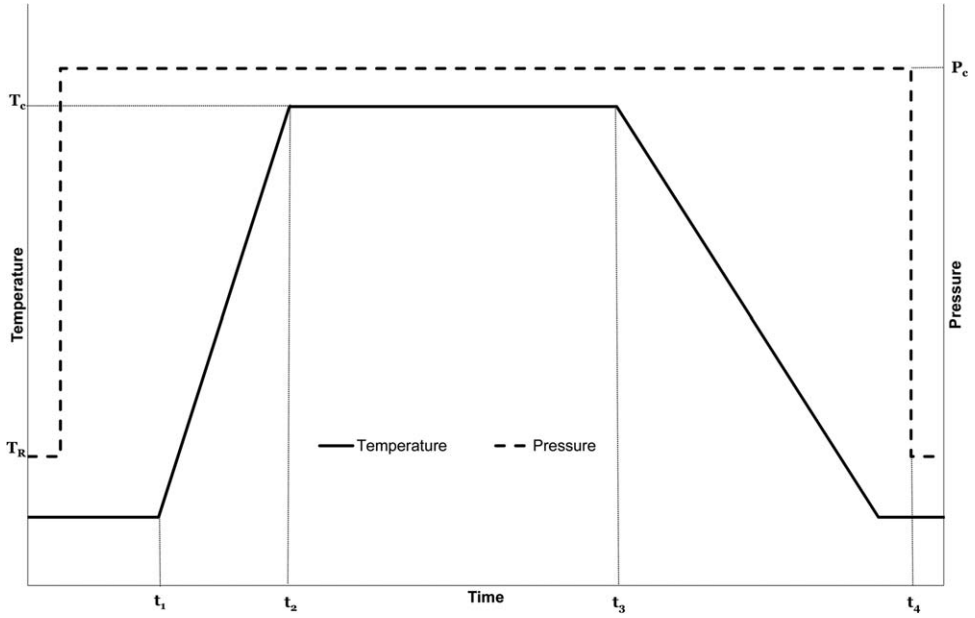

Figure 2. Manufacturing process temperature and pressure trends. T_C and P_C are respectively temperature and pressure applied during consolidation steady state (t_3–t_2). T_R is the room temperature.

Thermal Analysis

Differential scanning calorimetry (DSC) was performed on 5.5 mg samples taken from coextruded tape, using a Netzsch DSC 200 F3 Maia® differential scanning calorimeter. Homopolymer and copolymer behavior, within the temperature range used during consolidation, were evaluated. A three-step test was used: samples were first heated in the DSC from room temperature to 200 at 10°C min^{-1}, then cooled to 30°C at 10°C min^{-1} and finally heated to 200°C at 10°C min^{-1}. Data were collected during both heating phases and then compared in order to assess the temperature range where copolymer melts down.

Artificial Weathering

The system used for accelerated ageing was Q-Sun Xenon test Chamber Model Xe-1 manufactured by Q-LAB. The chamber was equipped with a xenon-arc lamp, which emitted radiation from ultraviolet to infrared. Considering the end use of all-PP materials a daylight filter was applied in order to produce a spectral power distribution (SPD) of 678.8 W m^{-2} in the range 300–800 nm equivalent to noon summer sunlight. An irradiance sensor and an insulated black panel temperature sensor, both embedded in the chamber, controlled the wavelength in the range 340 ± 10 nm and the temperature, respectively. Tests were conducted according to ISO 4892-part 2, Method A cycle n°2. An external water spray system was arranged to create rain conditions; the spray was pulsed 5 on and 55 s off for estimated water consumption of 1.0 L min^{-1} instantaneous and 0.08 L min^{-1} average. Only pure grade quality water produced by Merck Millipore Direct-Q® system was used during testing. Dark periods were introduced during water spray to simulate more realistic rain effect.

Raman Spectroscopy

Spectroscopic measurements were done using an in Via Raman system (Renishaw). The diode laser source operates at 785 nm, at 50% laser power and in single scan measurement mode. Four spectra were acquired at different areas in the range 125–3200 cm^{-1}.

RESULTS AND DISCUSSION

Coextruded tapes have been subjected to tensile tests to evaluate the mechanical properties of the laminate base constituents, since the influence of single tape performance on composite final properties was already demonstrated in literature.[10] Table II summarizes the main results. Plain weave fabric used in this work shows quite lower Young's modulus than commercially

Table I. Nomenclature Adopted for Laminates and Number of Tested Samples for Each Specimen Set

ID	Layer n°	T_C (°C)	t_C (s)	No. of tested samples
Consolidated laminates				
9_140_300	9	140	300	5
9_140_600	9	140	600	5
9_140_900	9	140	900	5
9_145_300	9	145	300	5
9_145_600	9	145	600	5
9_145_900	9	145	900	5
9_150_300	9	150	300	5
9_150_600	9	150	600	5
9_150_900	9	150	900	5
UV exposed laminates				
13_140	13	140	300	12
13_145	13	145	300	12
13_150	13	150	300	12

Table II. Characterization of Fabric Base Constituents: Single Tape Tensile Properties

Samples	Young's modulus (MPa)	Stress at break (MPa)	Strain at break (%)
Tape_1	4903	477	15.87
Tape_2	4699	401	13.24
Tape_3	4023	401	13.64
Tape_4	4264	417	13.13
Tape_5	4290	502	15.17
Mean	4436	440	14.21
Standard deviation	357	47	1.24

available material of similar type (~15 GPa at $\lambda = 17$) and comparable values of tensile strength.[10] This effect is probably due to orientation of crystalline and amorphous areas caused by lower draw ratios used in the coextrusion process.

When comparing the results reported in Table II with Figures 3 and 4, laminates consolidated at 140 and 145°C maintain tape original stiffness with a negligible variation of Young's modulus and fracture deformation.

Mechanical properties of samples consolidated at constant temperature are not influenced by the consolidation time (Figures 3–5). No substantial differences in Young's modulus and fracture stress values are observed for specimens manufactured at 140 and 145°C, but a slight decrease occurs when temperature approches 150°C. Parallel to this, fracture deformation does not vary for 9_140 and 9_145, whereas it increases for 9_150 (Figure 4). This consideration supports data illustrated in Figure 3 where analogous temperature dependence can be seen.

Results obtained for samples 9_150_300 shall be highlighted: Young's modulus and fracture stress drop significantly, while deformation increases up to 30%. This can be clearly seen in Figure 5, where four stress–strain curves of samples consolidated at 140, 145, and 150°C are shown. A comparative analysis of 9_140_300, 9_145_300 and 9_150_600 (Figure 5) underlines that material strength decreases and fracture deformation raises linearly as a function of consolidation temperature. The most interesting behavior is shown by sample 9_150_300 (red curve), which exhibits consistent strength drop and significant increase in fracture deformation. Reinforcement relaxation and localized melting are the mechanisms responsible for the peculiar behavior observed.

DSC analysis has been performed on the tapes to assess the operative temperature window, which is given by the difference between the homopolymer and copolymer melting temperatures. Two subsequent heating cycles have been adopted to investigate possible influences of the oriented nature of the core on the thermal behavior of the material. First heating (dashed line) and second heating (continuous line) are depicted in Figure 6.

The first heating is characterized by an endothermic peak at 107.3°C, which identifies the temperature where the copolymer starts to melt, followed by a pronounced peak at 166.4°C, typical of homopolymer. Around 150°C, a consistent broad peak characterizing the copolymer phase ultimate fusion is also visible.[19] This trend does not appear during the second heating since the material has lost its original structure, as confirmed by homopolymer peak shift from 166.4 to 163.7°C. Endothermic

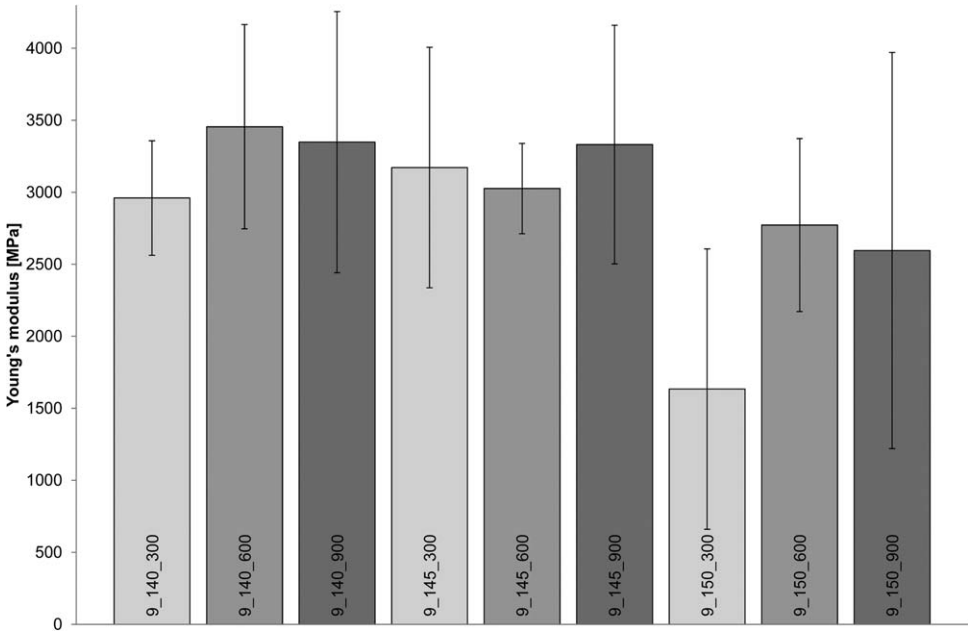

Figure 3. Tensile test results: laminate Young's moduli as a function of process parameters for the nine set of tested samples. Error bars indicate a 97% confidence interval.

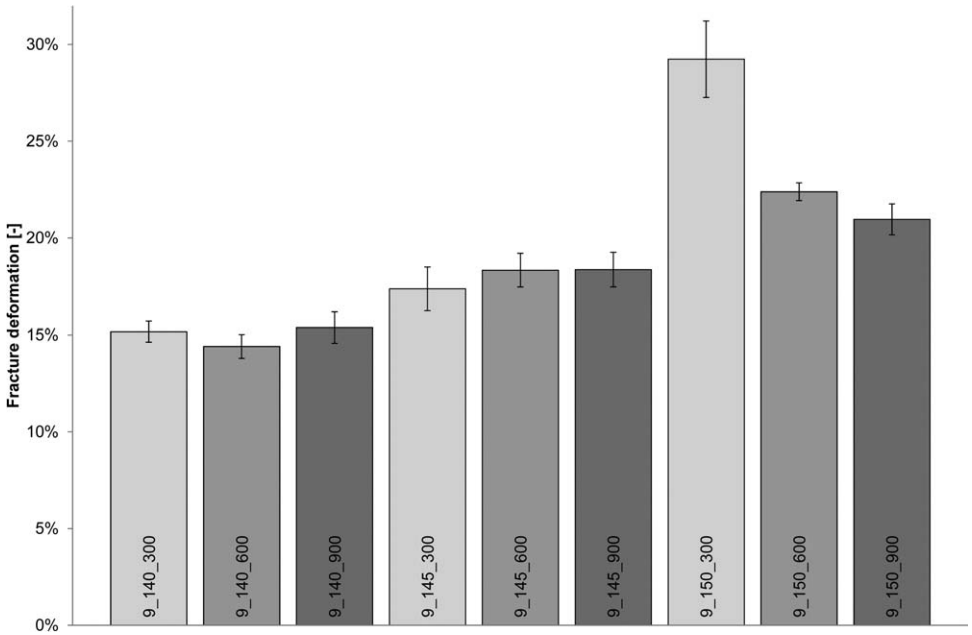

Figure 4. Tensile test results: laminate fracture deformation as a function of process parameters for the nine set of tested samples. Error bars indicate a 97% confidence interval.

curves overlap in the range 140–155°C results in difficult understanding of homopolymer and copolymer melting behavior. This implies that temperature should be controlled with high precision during manufacturing process to avoid relevant relaxation and localized melting in the oriented PP core.

Studies performed on analogous materials have demonstrated a wider temperature range suitable for thermoforming.[20,21] In particular, at 150°C PP tapes are subjected to selective fusion of the copolymer whereas the oriented core maintains its structure.

DSC analysis confirms that reinforcement relaxation and localized melting are the main causes for the mechanical property deterioration, as shown in Figure 5. The effect of temperature and insufficient pressure during consolidation induces oriented molecules to rearrange their structure in a more entropic configuration. Detrimental strength loss mentioned above has been

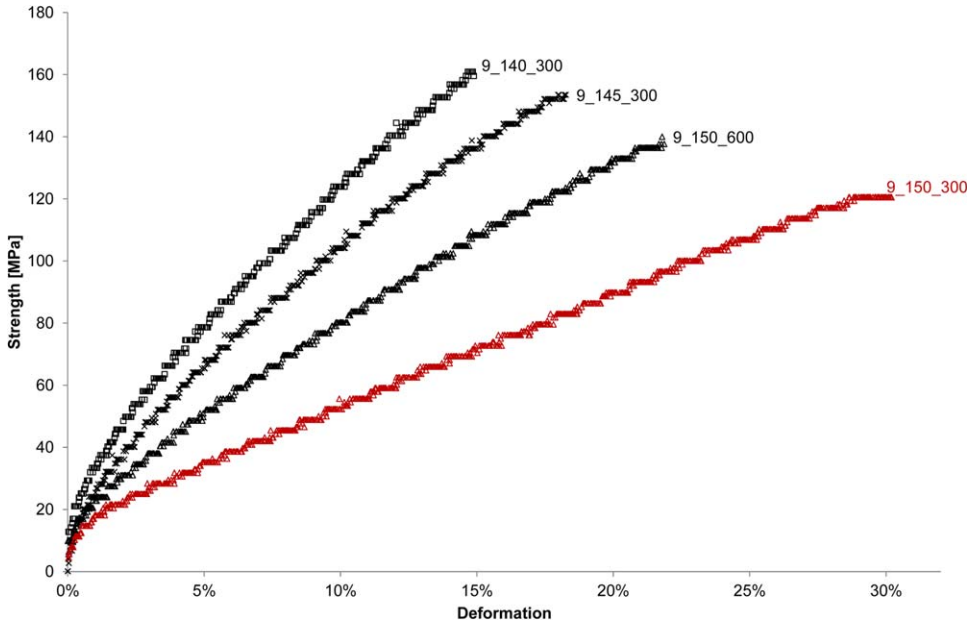

Figure 5. The stress–strain curves of laminates consolidated at 140, 145, and 150°C. 9_150_300 (red curve) shows a distinct trend respect to other curves. [Color figure can be viewed in the online issue, which is available at wileyonlinelibrary.com.]

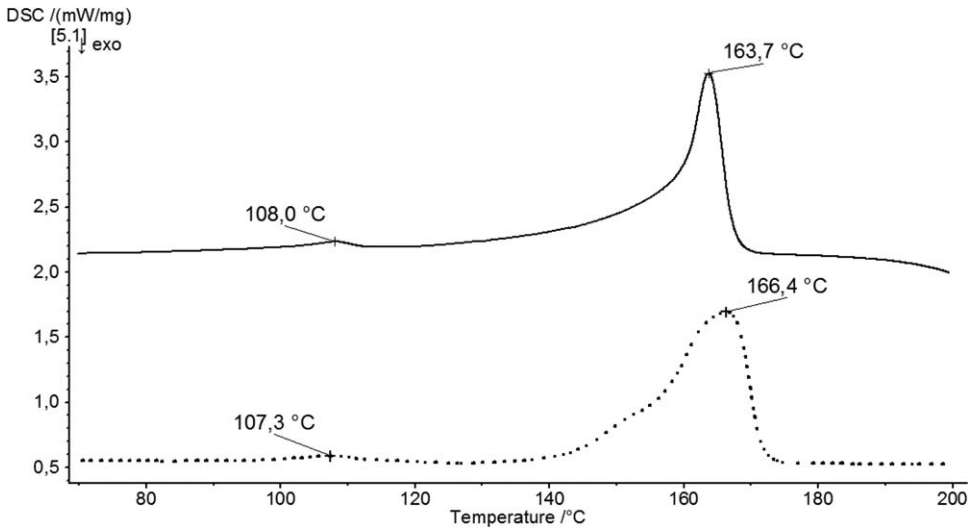

Figure 6. DSC analysis performed on single tape. Dashed line is representative of the first heating while continuous line depicts second heating. Curves have been detached to underline the differences.

occurred because in some areas temperature has been exceeded the onset of polypropylene core melting peak which has been calculated to be around 150°C.

Figures 7 and 8, where the surfaces of samples 9_140_300 and 9_150_300 subjected to tensile test are shown, support these considerations.

In Figure 7 detachment is visible at the boundary between tapes oriented in weft and warp direction; from the boundary, a set of parallel cracks spreads through the tape perpendicular to load axis. Micrograph in Figure 8 reveals a strong deformation of the tape on the right: in the same zone some bright areas suggest that partial melting and subsequent recrystallization has occurred.

Figure 9 summarizes the laminate tensile properties after artificial weathering as a function of ageing time. According to Figure 5, material strength reduces and fracture deformation increases as a function of processing temperature. Furthermore, all specimens show slight decrease of the mechanical properties when exposure time increases from 25 to 100 h, while a significant loss happens after 250 h. Pronounced reduction in fracture deformation, in particular for 13_150 after 100 h reveals a clear composite embrittlement. Figure 9 illustrates the relation between 13_140, 13_145, and 13_150 tensile properties with UV exposure time.

Figure 10 identifies the mechanism that leads to premature failure. After 250 h of exposure, wide delamination occurs while there is an 85% deformation drop for 13_140, 81% for 13_145 and 88% for 13_150, respectively.

The micrograph illustrating the surface of 13_140 sample (Figure 11) shows detached interfaces between tapes oriented in

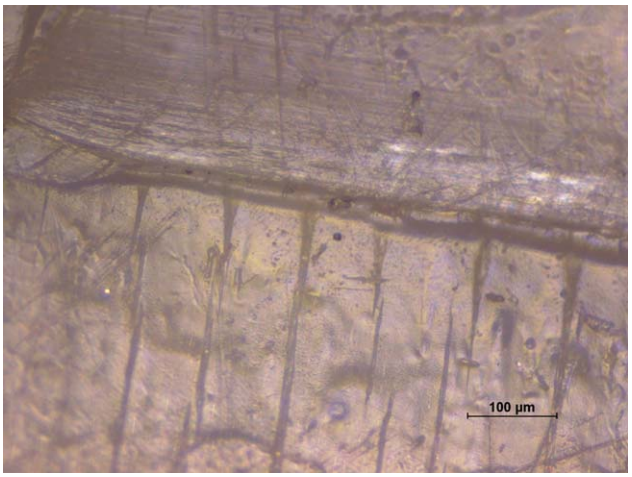

Figure 7. The optical micrograph (10× Nikon Eclipse 50i) of 9_140_300 after tensile test identifies the detached interface between tapes and vertical intratape cracks caused by load. [Color figure can be viewed in the online issue, which is available at wileyonlinelibrary.com.]

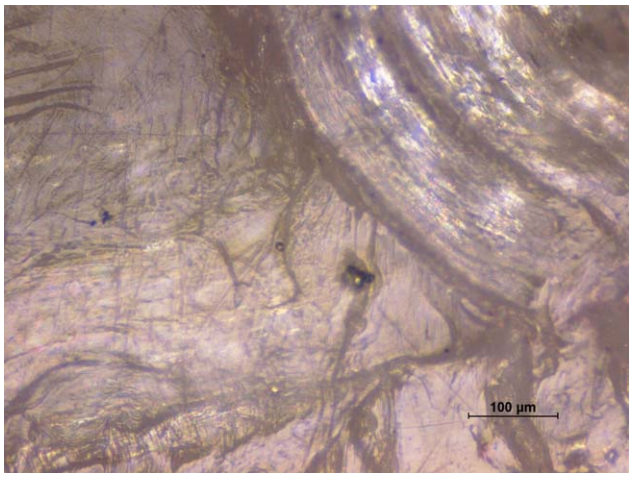

Figure 8. The optical micrograph (10× Nikon Eclipse 50i) of 9_150_300 after tensile test shows material plastic flow induced by load. [Color figure can be viewed in the online issue, which is available at wileyonlinelibrary.com.]

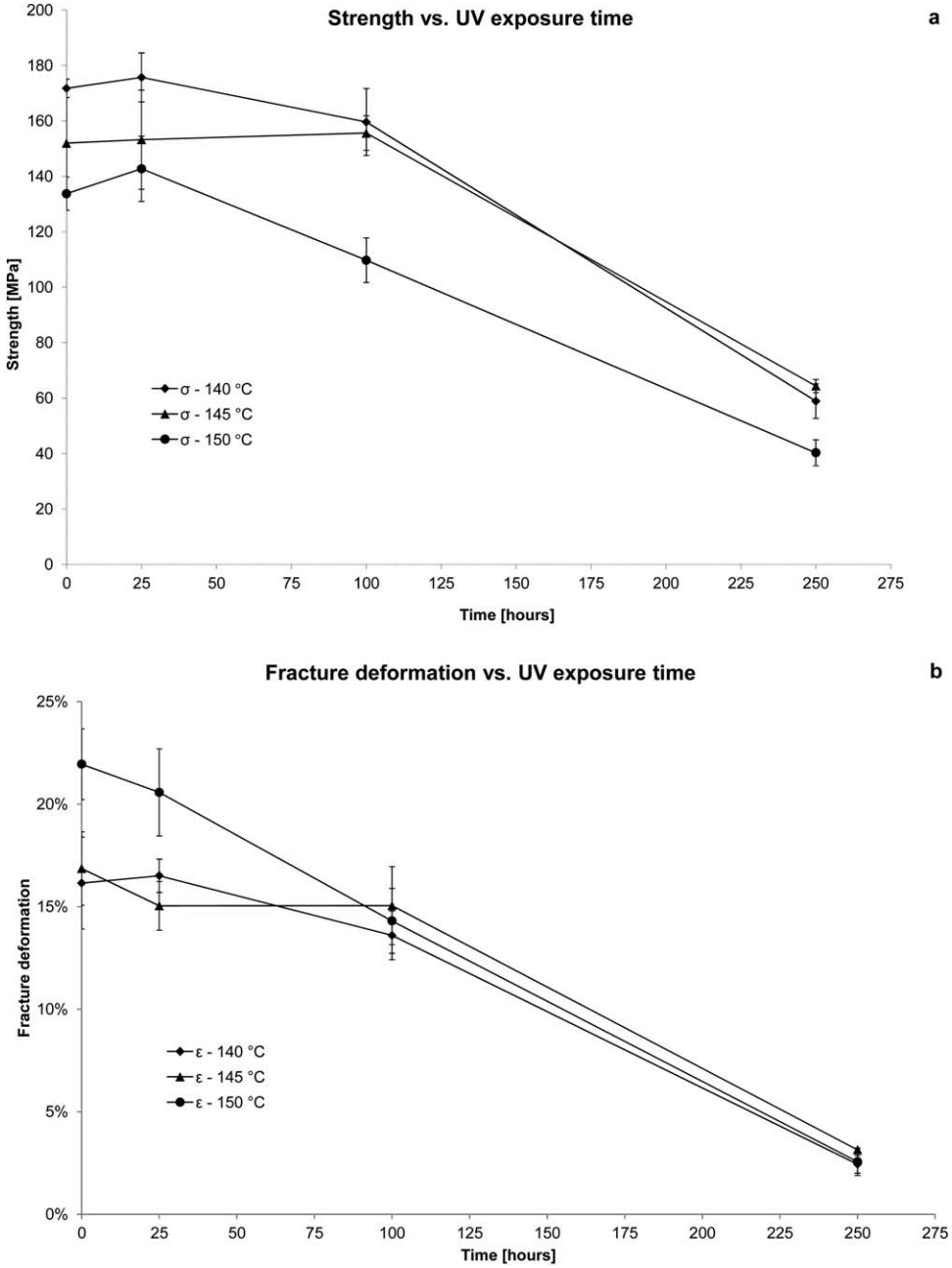

Figure 9. All-PP composite strength (a) and fracture deformation (b) versus exposure time for 13_140, 13_145 and 13_150. It is clearly visible a dramatic drop of mechanical performance (a) and fracture deformation (b).

weft and warp direction and microcracks induced by UV radiation in the middle left. This suggests that UV light weakens mainly areas that have reached melting during thermoforming, promoting cohesive fracture propagation within this phase.

Figure 12 compares the spectra acquired on the surface of sample 13_140 subjected to 50 (line black) and 125 h of irradiation (line red and blue). It is noteworthy that all samples have been regularly capsized during artificial weathering and so each surface has been irradiated for half the time with respect to those reported in Figure 9. Blue and red spectra have been collected in the areas shown by the arrows in Figure 11. Raman spectrum of specimen aged for 125 h shows different spectral features between 630 and 685 cm^{-1} and from 1530 and 1770 cm^{-1}. These peaks correspond to the carbonyl group's vibration modes, which are typical of carboxylic acids (1700–1720 cm^{-1}) and esters (1770 cm^{-1}). These vibrational modes formed due to the influence of time exposing light.[22] The weak band between 630–685 and 1500–1550 cm^{-1} could represent the secondary vibration modes of the carbonyl group, which are typical of diketones and aldehydes. Red and blue spectra have been measured on contiguous areas on the same

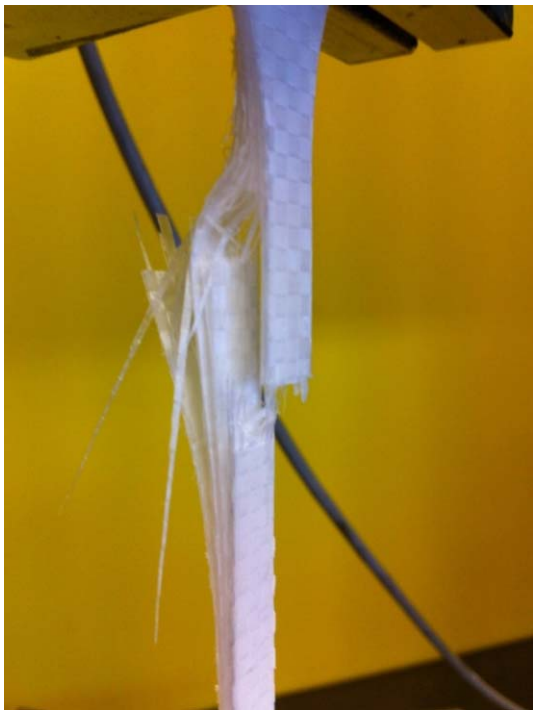

Figure 10. Brittle fracture mechanism of samples 13_140 conditioned for 250 h. The image depicts noticeable delamination and considerable reduction of tape fibrillation. [Color figure can be viewed in the online issue, which is available at wileyonlinelibrary.com.]

sample and they support the fact that areas brought to fusion during consolidation (matrix) are prone to the detrimental effect of UV radiation.

As mentioned in previous work, peroxides characteristic double bands in the range 1805–1780 and 1785–1755 cm^{-1} have not been found because of their instability.[12,23] The formation of

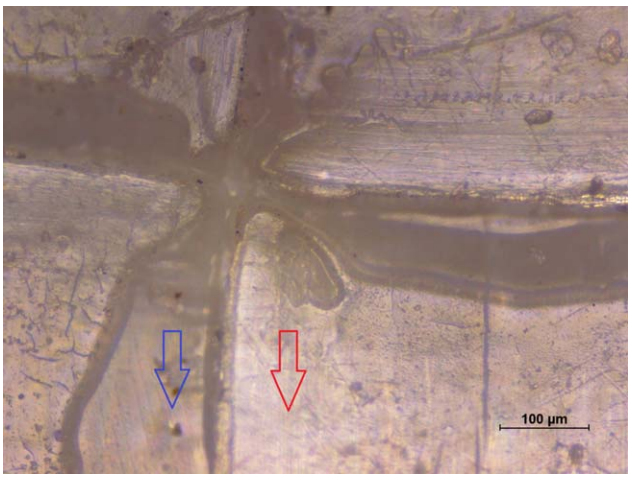

Figure 11. The optical micrograph (10× Nikon Eclipse 50i) of 13_140 surface shows intersection between tapes oriented in weft (vertical) and warp (horizontal) direction. Blue and red arrows specify areas analyzed by Raman spectroscopy. [Color figure can be viewed in the online issue, which is available at wileyonlinelibrary.com.]

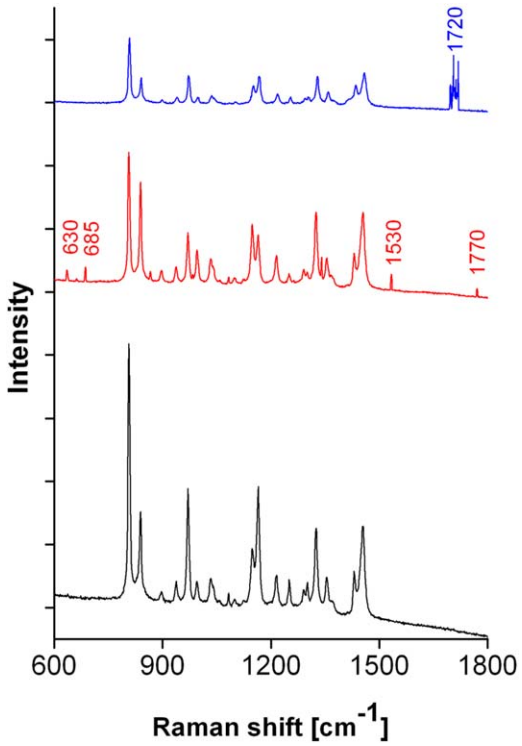

Figure 12. Comparison between Raman spectra: 13_140 after 50 h (black) and after 125 h but in different position (blue and red). Blue and red spectra refer to positions marked in Figure 11. [Color figure can be viewed in the online issue, which is available at wileyonlinelibrary.com.]

low molecular weight by-products confirms the reduction of mechanical properties shown in Figure 9.

CONCLUSIONS

The mechanical properties of coextruded tapes have been measured and the influence of processing parameters on all-PP composites have been investigated to describe the behavior of this class of materials. Consolidation time does not modify significantly the mechanical properties, while temperature should be strictly controlled to obtain laminates with superior performance. As demonstrated by DSC measurements, temperature is the major cause of molecular relaxation and selective melting of the surface during processing. Furthermore, weathered all-PP composite tensile properties have been evaluated and a qualitative determination of by-products resulting from photo-oxidation process has been assessed using spectroscopic technique. After 100 h of exposure, only a slight strength reduction has been noted. On the other hand, samples that were conditioned for 250 h have shown matrix embrittlement and significant strength loss. Results collected from Raman spectra have confirmed the presence of several species of the carbonyl group.

ACKNOWLEDGMENTS

This work have been developed inside INDUSTRIA 2015—Sustainable Mobility project funded by MISE (Italian Ministry of Economic Development) which is gratefully acknowledged for financial support. The authors would like to thank Stefano

Pasqualin for his very precious cooperation in sample preparation. All tests have been conducted using facilities at University of Trieste.

REFERENCES

1. Alcock, B.; Cabrera, N. O.; Barkoula, N. M.; Spoelstra, A. B.; Loos, J.; Peijs, T. *Compos. A* **2007**, *38*, 147.
2. Alcock, B.; Cabrera, N. O.; Barkoula, N. M.; Loos, J.; Peijs, T. *Compos. A* **2006**, *37*, 716.
3. Peijs, T. *Mater. Today* **2003**, *6*, 30.
4. Kmetty, A.; Bárány, T.; Karger-Kocsis, J. *Prog. Polym. Sci.* **2010**, *35*, 1288.
5. Houshyar, S.; Shanks, R. A.; Hodzic, A. *Macromol. Mater. Eng.* **2005**, *290*, 45.
6. Ward, I. M.; Hine, P. J. *Polymer* **2004**, *45*, 1423.
7. Hine, P. J.; Ward, I. M.; Jordan, N. D.; Olley, R.; Bassett, D. C. *Polymer* **2003**, *44*, 1117.
8. Hine, P. J.; Ward, I. M.; Teckoe, J. *J. Mater. Sci.* **1998**, *33*, 2725.
9. Jordan, N. D.; Bassett, D. C.; Olley, R. H.; Hine, P. J.; Ward, I. M. *Polymer* **2003**, *44*, 1133.
10. Alcock, B.; Cabrera, N. O.; Barkoula, N. M.; Peijs, T. *Eur. Polym. J.* **2009**, *45*, 2878.
11. Deng, H.; Reynolds, C. T.; Cabrera, N. O.; Barkoula, N. M.; Alcock, B.; Peijs, T. *Compos. B Eng.* **2010**, *41*, 268.
12. Aslanzadeh, S.; Kish, M. H. *Fiber Polym.* **2010**, *11*, 710.
13. Yang, X.; Ding, X. *Geotext. Geomembr.* **2006**, *24*, 103.
14. Arruebarrena de Báez, M.; Hendra, P. J. Judkins, M. *Spectrochim. Acta A Mol. Biomol. Spectr.* **1995**, *51*, 2117.
15. Gen, D. E.; Prokhorov, K. A.; Nikolaeva, G. Y.; Sagitova, E. A.; Pashinin, P. P.; Shklyaruk, B. F.; Antipov, E. M. *Laser Phys.* **2011**, *21*, 125.
16. Chernyshov, K.; Gen, D.; Shemouratov, Y.; Prokhorov, K.; Nikolaeva, G.; Sagitova, E.; Pashinin, P.; Kovalchuk, A.; Klyamkina, A.; Nedorezova, P.; Shklyaruk, B.; Optov, V. *Macromol. Syst.* **2010**, *296*, 505.
17. Blakey, I.; George, G. A. *Polym. Degrad. Stabil.* **2000**, *70*, 269.
18. Sato, H.; Shimoyama, M.; Kamiya, T.; Amari, T.; Aic, S.; Ninomiya, T.; Siesler, H. W.; Ozaki, Y. *J. Appl. Polym. Sci.* **2002**, *86*, 443.
19. Alcock, B.; Cabrera, N. O.; Barkoula, N. M.; Loos, J.; Peijs, T. *J. Appl. Polym. Sci.* **2007**, *104*, 118.
20. Kitayama, T.; Utsumi, S.; Hamada, H.; Nishino, T.; Kikutani, T.; Ito, H. *J. Appl. Polym. Sci.* **2003**, *88*, 2875.
21. Houshyar, S.; Shanks, R. A. *Macromol. Mater. Eng.* **2003**, *288*, 599.
22. Popa, M. I.; Pernevan, S.; Sirghie, C.; Spiridon, I.; Chambre, D.; Copolovici, D. M.; Popa, N. *J. Chem.* **2013**, article number: 343068.
23. Chenery, D. H. *Biomaterials* **1997**, *18*, 415.